Journal of Physics: Theories and Applications E-ISSN: 2549-7324 / P-ISSN: 2549-7316
J. Phys.: Theor. Appl. Vol. 9 No. 2 (2025) 133-147 doi: 10.20961/jphystheor-appl.v9i2.108090

Photoacoustic imaging of oil-treated tissues for the potential support of halal product identification

Putut Giri Tulus Widodo[1], Mitrayana[1*]

[1]Department of Physics, Universitas Gadjah Mada

mitrayana@mail.ugm.ac.id

Received 14 August 2025, Revised 28 August 2025, Published 30 September 2025

Abstract: Photoacoustic Imaging (PAI) has successfully demonstrated its capability as a non-destructive method for distinguishing biological tissues based on oil absorption characteristics. Chicken meat samples were soaked in coconut oil, sesame oil, and lard for 10 minutes, 60 minutes, and 24 hours. The PAI system employed a 532 nm green laser, condenser microphone, and a two-dimensional scanning stage to capture spatial images. Grayscale and pseudocolor images were analyzed to extract numerical features including mean intensity, standard deviation, and entropy. Results showed that tissues treated with lard consistently exhibited higher values of numerical feature, particularly after 24 hours, compared to samples with vegetable oils. These variations are linked to stronger optical absorption and increased structural complexity caused by oil infiltration. The study demonstrates that PAI can effectively detect oil-specific changes in tissue, suggesting its potential role in supporting halal product verification.

Keyword: Photoacoustic, coconut oil, sesame oil, lard, entropy, non-destructive method

1. Introduction

Photoacoustic imaging (PAI) is a hybrid modality that synergistically integrates the contrast advantages of optical imaging with the spatial resolution of ultrasound. The method relies on the photoacoustic effect, where pulsed laser light is absorbed by tissue chromophores, resulting in rapid thermoelastic expansion and the emission of ultrasonic waves. These waves are then detected to reconstruct spatial maps of optical absorption properties within biological samples (Hu, 2012) (Beard, 2011). Because the generated acoustic signals are directly related to the optical absorption properties of biological chromophores, PAI enables detailed visualization of endogenous molecules such as hemoglobin, melanin, and lipids with high spatial resolution.

One promising application of PAI is the analysis of oil-induced alterations in biological tissues, as the technique demonstrates high sensitivity to the presence and optical absorption characteristics of lipid-based substances. This capability opens new possibilities for compositional analysis, including the differentiation of biological samples exposed to oils of various origins, which is potentially relevant for supporting halal product identification. Recent studies have demonstrated that photoacoustic-based

techniques can provide molecular-level information about lipid composition and its degradation. For example, spectral analysis-assisted PAI has been employed to differentiate cholesterol, fat, and olive oil in tissue-mimicking phantoms by leveraging subtle variations in spectral time-of-flight signatures (Cao at al., 2017). Moreover, photoacoustic spectroscopy (PAS) has been successfully applied to monitor thermal-induced chemical changes in edible oils, detecting spectral shifts associated with the breakdown of unsaturated fatty acids without the need for chemical pretreatment (Albuquerque at al., 2013). These findings support the use of PAI and PAS as non-destructive approaches for compositional lipid analysis, which aligns with efforts to verify oil origin in biological samples.

Photoacoustic images encode optical absorption contrast into grayscale intensities, where pixel values reflect local tissue properties. These can be quantified using statistical features such as mean, standard deviation, contrast, and entropy. Mean and standard deviation capture overall brightness and variability; contrast reflects dynamic range; while entropy indicates structural complexity and randomness (Zhao at al., 2014).

These features are particularly useful in differentiating tissue exposed to various oils. When tissues are soaked in oils with distinct lipid compositions, their absorption characteristics change, affecting the resulting image texture. Saturated or viscous oils tend to increase entropy and standard deviation due to uneven diffusion and localized scattering (Balasundaram at al., 2020).

The composition of cooking oil can affect both public health and individual dietary needs, such as halal food compliance. Certain oils are rich in saturated or trans fats, which are associated with increased cardiovascular risk (Ronald P Mensink, 2003). In halal dietary systems, it is crucial to distinguish animal-derived oils, as ingredients from non-halal sources are prohibited (Mensink at al., 2003; Belkhatir at al., 2020.). The growing attention to halal food integrity, supported by regulatory bodies and consumer awareness, reflects an urgent need for transparent verification systems (Anggraini at al., 2023). Therefore, analytical methods that can determine oil origin in food or biological matrices are increasingly relevant for maintaining both health standards and halal authenticity. While chemical analysis remains a standard method, optical-based, non-destructive approaches such as PAI are underexplored.

In this study, a photoacoustic imaging (PAI) system was employed to capture grayscale images of biological tissue samples subjected to three different oil treatments: coconut oil, sesame oil, and lard. The samples consisted of chicken meat soaked in each oil type to simulate oil absorption under controlled conditions. After image acquisition, quantitative texture features were extracted from the resulting images, focusing on statistical descriptors such as standard deviation, global entropy, and local entropy. Standard deviation measures the overall dispersion of pixel intensities, indicating brightness variability across the image. Global entropy quantifies the randomness of intensity distribution, reflecting the complexity of tissue structure (Zhao at al., 2014). Multiscale entropy, along with complexity texture analysis, has been proposed to account for the multiple time scales inherent in biological signals (Yeh at al., 2011).

Previous studies have primarily focused on identifying lipid content in tissue using spectroscopic or chemical analysis. However, limited research has explored the application of photoacoustic imaging to detect structural and optical differences in tissue exposed to oils of different halal status, particularly using quantitative texture analysis approaches such mean intensity, standard deviation, global entropy, and local entropy mapping. This study aims to address this gap by investigating the use of PAI to differentiate between chicken tissue samples soaked in coconut oil, sesame oil, and lard under various time exposures.

2. Methods

2.1. Photoacoustic Imaging System

The photoacoustic imaging (PAI) system used in this study was a laboratory-built setup developed at the Applied Physics Laboratory, Universitas Gadjah Mada. The system operates based on the photoacoustic effect. In this process, pulsed laser light is first absorbed by chromophores within the tissue, which leads to rapid localized heating. This thermal energy induces thermoelastic expansion, producing broadband acoustic waves that propagate through the tissue. These pressure waves are detected using a Behringer ECM8000 condenser microphone, which has sensitivity in the 20–20,000 Hz range, suitable for detecting acoustic signals generated from biological samples. The acoustic signals are digitized via an external USB sound card, then processed using a LabVIEW-based interface for signal acquisition and reconstruction.

Optical excitation is provided by a 532 nm green diode laser, modulated via transistor-transistor logic (TTL) pulses generated by an Arduino Uno microcontroller. The laser output operates in continuous wave (CW) mode, with modulation frequency and duty cycle adjustable through software.

A mechanical XY-scanning stage, driven by Nema-17 bipolar stepper motors and controlled via an Arduino Nano, allows automated two-dimensional scanning of the sample area. The smallest step resolution of the motors is approximately 1.8° per step, and the scanning area covers approximately 30 mm × 30 mm. Samples are positioned on a custom holder within an imaging chamber filled with distilled water to provide acoustic coupling.

To ensure system accuracy and replicability, several supporting instruments were used. A Optical Power Meter was employed to measure the laser output power for calibration. Additionally, a function generator was used during the microphone characterization phase to generate acoustic signals at specific frequencies, enabling assessment of the microphone's response behavior. A schematic of the system is shown in Figure 1.

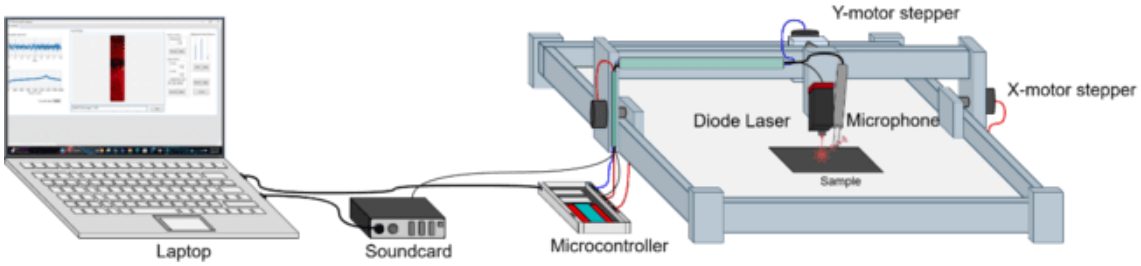

Figure 1. Schematic of the photoacoustic imaging system used to acquire images of oil-treated chicken tissue samples.

Theoretical modeling of the photoacoustic signal generation follows standard formulation (Paltauf at al., 2018). The initial pressure distribution $p_0(r)$ generated in the tissue is given by:

$$p_0(r) = \boldsymbol{\Gamma}\, \mu_a(r)\, \Psi(r)$$

where $\boldsymbol{\Gamma}$ is the Gr¨uneisen parameter (assumed constant), $\mu_a(r)$ is the optical absorption coefficient, and $\Psi(r)$ is the optical fluence at position r. This initial pressure acts as the source of the acoustic wave. The time-resolved pressure at a detection point r_0 is expressed as:

$$p_0(r,t) = \frac{\beta}{4\pi Cp}\frac{\partial y}{\partial x}\int_V W(r)\ \frac{1}{|r_0 - r|}\ \delta\left(t - \frac{|r_0 - r|}{c_s}\right) d^3\, r$$

where β is the thermal expansion coefficient, Cp is the specific heat at constant pressure, cs is the speed of sound in the medium, and $W\ (r)\ =\ \mu_a(r)\Psi(r)$ is the absorbed energy density (Paltauf at al., 2018).

The detected signal $s(r_d, t)$ is modeled as:

$$s(r_d, t) = \int_V\ W(r)\ h\ (r_d, r, t)\ d^3 r,$$

where $h(r_d, r, t)$ is the system's spatiotemporal impulse response, composed as:

$$h\ =\ g_{att}\ *\ g_{el}\ *\ g_{pa}\ *\ g_s,$$

with g_{att} accounting for acoustic attenuation, g_{el} the detector's electrical response, g_{pa} the photoacoustic point source response, and g_s spatial impulse response (Paltauf at al., 2018).

In this experiment, fresh boneless chicken breast was cut into uniform cubes measuring approximately 1 × 1 × 1 cm. Each sample was fully immersed in 10 mL of one type of cooking oil (coconut oil, sesame oil, or lard) for 10 minutes, 60 minutes, or 24 hours at room temperature (25 ± 1 °C). To ensure consistency, all samples were identical in size and were placed in closed containers during immersion to prevent contamination. These immersion times were chosen to simulate short, intermediate, and prolonged exposure levels that may influence lipid absorption profiles in biological tissues. After soaking, samples were gently blotted to remove surface oil before imaging. A schematic of the sample preparation process is shown in Figure 2.

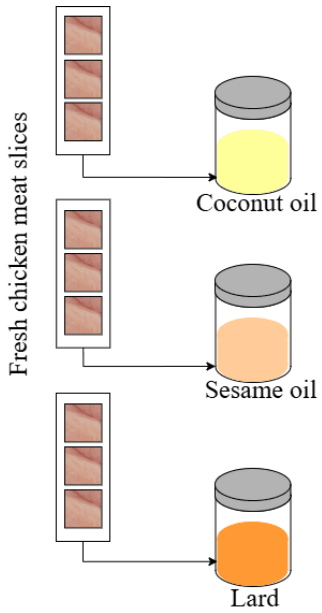

Figure 2: Schematic of the sample preparation process. Fresh chicken meat slices were soaked in three different cooking oils: coconut oil, sesame oil, and lard, for durations of 10 minutes, 60 minutes, and 24 hours. The treated samples were then prepared for photoacoustic imaging to evaluate the effect of oil absorption.

For image acquisition, after the sample was prepared, each sample was placed individually on the scanning stage and aligned under the detection area for image acquisition. For each sample, the scanning process was initiated through the Photoacoustic Imaging Software, which allowed for precise control of laser modulation parameters including frequency and duty cycle. Before scanning, these parameters were adjusted to optimal values through the application's interface to ensure consistent excitation conditions across all samples.

Once parameters were set, the sample was scanned in a two-dimensional raster pattern by the XY-motor stage, and the photoacoustic signals were continuously recorded. The detected acoustic signals, corresponding to localized optical absorption, were converted into grayscale intensity maps representing spatial variations in tissue properties. These images were automatically saved in matrix format on the connected computer.

The acquisition process generated pseudocolor and grayscale photoacoustic images that visualized the spatial distribution of optical absorption within the tissue samples. Pseudocolor images facilitated qualitative interpretation by highlighting structural variations such as brightness gradients and texture patterns across different oil treatments. Grayscale images were used for quantitative analysis. These grayscale images were then processed numerically to extract statistical features that characterize intensity variation and texture complexity. Specifically, mean intensity, standard deviation, and entropy were computed to evaluate the influence of oil type and immersion duration on tissue properties. The next section presents the detailed methodology of image analysis, including the extraction and interpretation of these descriptors.

2.2. Image Analysis

Following photoacoustic acquisition, numerical analysis was performed on the resulting grayscale images using Google Colab with Python libraries such as NumPy, PIL, Pandas, and Matplotlib to extract statistical features that may serve as distinguishing parameters. Image-based features provide insights into underlying structural and compositional differences that are not readily visible in raw images. Commonly used descriptors in image-based analysis include intensity mean, standard deviation, entropy, and local texture indices, which help quantify image variability, texture complexity, and spatial heterogeneity.

In this study, we focused on three quantitative descriptors: mean intensity, standard deviation, and entropy. Mean intensity represents the average brightness level in the image, reflecting the overall optical absorption of the tissue. Standard deviation captures the spread of pixel intensity values, providing a measure of image uniformity and intensity variation. Entropy is a well-established metric frequently used to assess the complexity and non-uniformity of image texture (Zhao at al., 2014). In the diagnosis of pulmonary nodules, for example, malignant lesions have been shown to exhibit significantly higher entropy than benign ones, demonstrating entropy's capacity to reflect meaningful structural variation (Zhao at al., 2014; Zhang at al., 2021).

Two-dimensional entropy (TE) is a statistical measurement that captures local information in an image by considering the spatial correlation between a center pixel and its neighbors. Unlike 1D entropy, TE takes into account feature pairs composed of the center pixel value and the average of its eight neighbors, making it more sensitive to local structures and spatial distributions. TE is computed from the joint probability distribution of the center gray level (x_1) and the average of the surrounding eight pixels (x_2), based on the frequency of the pair (x_1, x_2). The two-dimensional entropy is defined as:

$$H_2(x) = -\sum_{x_1=0}^{255} \sum_{x_2=0}^{255} p(x_1, x_2)\, log_2\, p(x_1, x_2)$$

To complement global entropy analysis, we generated local entropy maps using a sliding window of 9×9 pixels, allowing visualization of regional texture variations across the tissue surface. This approach improves sensitivity to localized structural differences and has been applied effectively in biomedical imaging contexts (Hrvzic at al., 2019). By comparing both the values and spatial distributions of standard deviation and entropy across treatment groups, we observed that oil type and immersion duration produced consistent and quantifiable differences in photoacoustic image characteristics.

3. Results and Discussion

To assess the effects of oil type and immersion duration on tissue optical properties, psudocolor and grayscale photoacoustic images were acquired from nine chicken meat samples. Each sample was treated with one of three cooking oils: coconut oil (CO), sesame oil (SO), or lard for varying durations (10, 60, and 24 minutes). As shown in

Figure 3, visual differences in tissue surface coloration were already apparent after treatment.

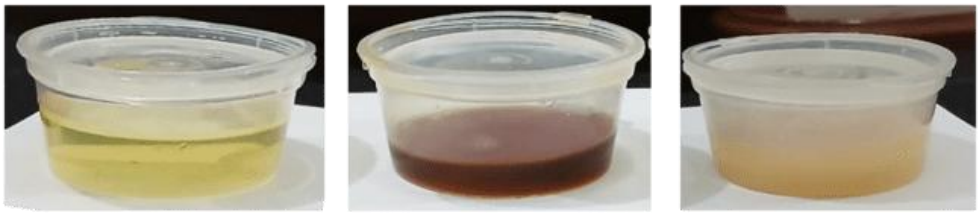

Figure 3: Visual documentation of chicken meat samples immersed in (a) coconut oil, (b) sesame oil, and (c) lard, for 10 minutes, 60 minutes, and 24 hours.

The acquired photoacoustic images revealed contrast variations that reflect changes in tissue structure due to oil absorption. All samples were imaged using a standardized setup with a 532 nm diode laser, which primarily excites endogenous chromophores such as myoglobin and hemoglobin. Although lipids exhibit weak absorption at this wavelength, the presence of oil within the tissue appears to affect light scattering, modify optical fluence distribution, and displace native chromophores. These combined effects contribute to variations in photoacoustic signal patterns across samples.

Lard-treated tissues, even after short immersion, showed enhanced structural heterogeneity and sharper signal gradients compared to samples soaked in coconut or sesame oil. This suggests that animal-based fats may penetrate tissue more effectively or reorganize internal structures differently than plant-based oils. These results are consistent with prior findings by Balasundaram et al. (2020), who reported that lipid-rich regions produced higher contrast in optoacoustic images due to altered scattering and absorption. Our findings therefore support the hypothesis that oil composition plays a significant role in tissue–oil interaction, which can be visualized non-invasively using PAI.

Pseudocolor visualizations of the photoacoustic images demonstrate progressive structural changes in tissue samples depending on oil type and immersion duration. After 10 minutes of soaking, as shown in the pseudocolor image of Figure 4, the tissue treated with lard already displays greater textural heterogeneity and more pronounced edge gradients than those treated with coconut oil or sesame oil. This observation suggests initial surface-level infiltration or localized interaction between saturated animal fat and the tissue matrix.

With extended immersion of 60 minutes, the differences between oil treatments become more evident. As displayed in Figure 5, the lard-treated tissue exhibits broader spatial gradients and increased internal variation, indicating more substantial oil penetration and disruption of tissue microstructure. In contrast, tissues immersed in coconut and sesame oil remain visually more homogeneous, with only minor deviations from their earlier appearance, suggesting limited oil diffusion over time.

After 24 hours of immersion, the visual distinctions reach their peak. The pseudocolor image presented in Figure 6 shows that the lard-treated tissue has developed widespread signal irregularity, distinct internal patterning, and marked structural complexity. These

changes are likely caused by the redistribution of chromophores, deeper lipid infiltration, and altered light scattering behavior. Meanwhile, tissues treated with coconut and sesame oil continue to appear more uniform and symmetric. These visual outcomes support the hypothesis that animal-derived oils induce more aggressive optical and structural changes in tissue compared to plant-based oils. Similar trends in contrast and spatial variation have been reported in previous photoacoustic research involving lipid-rich media, such as those described by Balasundaram et al. (2020).

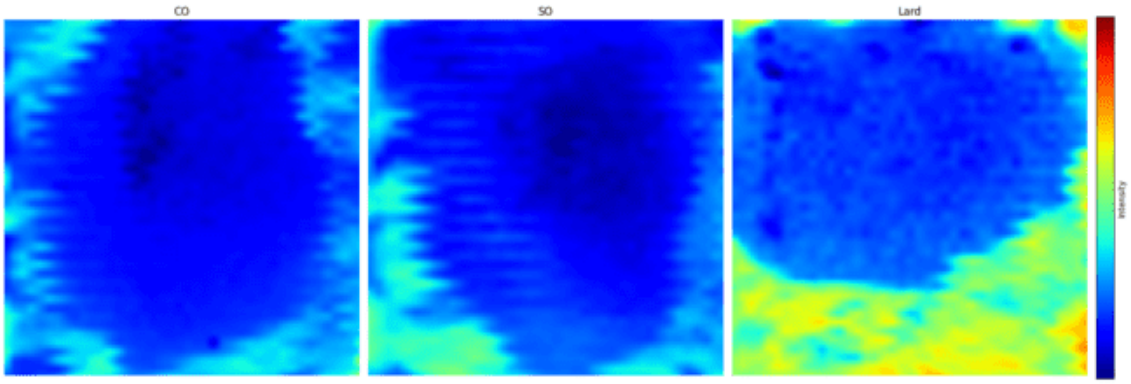

Figure 4: Pseudocolor photoacoustic images of tissue samples after 10-minute immersion in (from left to right) coconut oil, sesame oil, and lard. Blue areas represent tissue signal; red areas represent background.

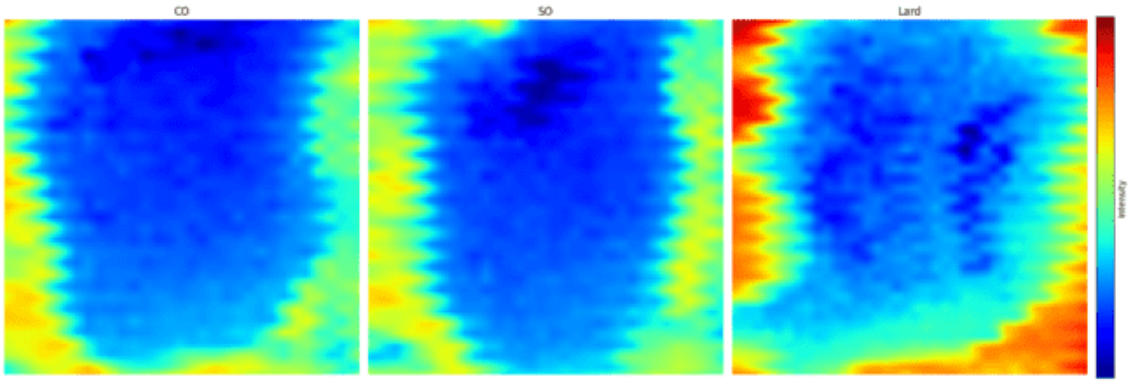

Figure 5: Pseudocolor photoacoustic images of tissue samples after 60-minute immersion in (from left to right) coconut oil, sesame oil, and lard.

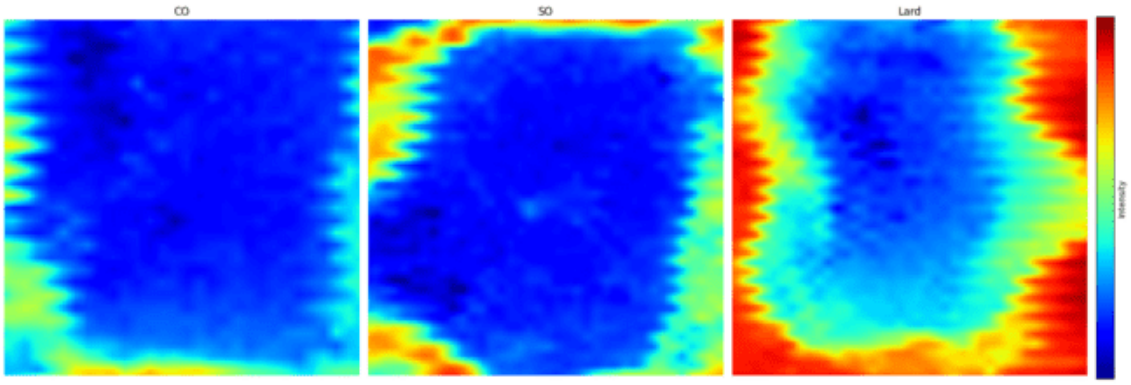

Figure 6: Pseudocolor photoacoustic images of tissue samples after 24-hour immersion in (from left to right) coconut oil, sesame oil, and lard.

Although all samples were imaged under identical conditions using a 532 nm green laser, the resulting photoacoustic contrasts vary considerably depending on the type of oil and duration of immersion. The tissue samples treated with lard exhibited stronger and more heterogeneous signals, especially after prolonged exposure. These observations confirm that photoacoustic imaging is not only sensitive to endogenous chromophore absorption, such as myoglobin and hemoglobin, but also responsive to structural and compositional changes introduced by external agents like oil. The visual differences highlighted earlier provide a compelling basis for further quantitative analysis aimed at characterizing tissue-oil interactions through measurable image features.

To validate the visual differences observed across oil treatments and immersion durations, we performed a quantitative analysis of the grayscale photoacoustic images. The same Python-based workflow described earlier was applied to extract numerical features that provide objective insights into the underlying structural variations. Rather than relying solely on subjective visual cues, this statistical approach enables the measurement of signal intensity, contrast distribution, and texture complexity. These metrics, previously defined, form the foundation for discriminating between oil-treated samples and for evaluating their classification potential in non-invasive applications.

A complete set of grayscale photoacoustic images is shown in Figure 7, presenting the visual outcomes for each combination of oil type and immersion duration. These images offer a more neutral, intensity-preserving view of optical absorption patterns across the tissue surface, with coconut oil, sesame oil, and lard treatments arranged sequentially at 10 minutes, 60 minutes, and 24 hours. Although less visually striking than the pseudocolor renderings, the grayscale images retain essential intensity information that serves as the basis for statistical analysis.

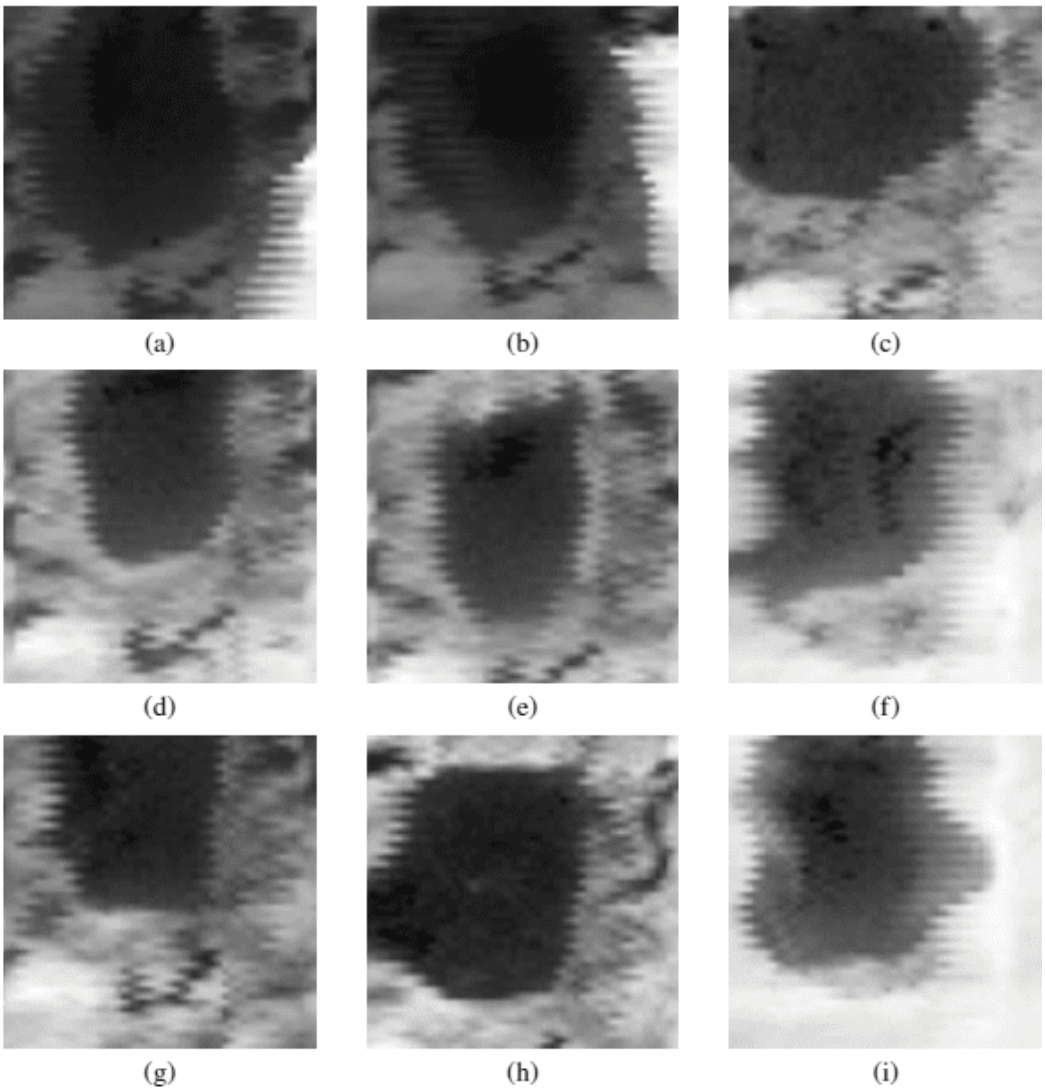

Figure 7: Grayscale photoacoustic images of chicken tissue samples treated with different cooking oils. (a) Coconut oil, 10 minutes; (b) Sesame oil, 10 minutes; (c) Lard, 10 minutes; (d) Coconut oil, 60 minutes; (e) Sesame oil, 60 minutes; (f) Lard, 60 minutes; (g) Coconut oil, 24 hours; (h) Sesame oil, 24 hours; (i) Lard, 24 hours.

Table 1 to Table 3 present the quantitative results for immersion durations of 10 minutes, 60 minutes, and 24 hours, respectively. In each case, the lard-treated samples consistently show higher mean intensity, greater standard deviation, and higher entropy values compared to those treated with coconut oil and sesame oil. This trend becomes more pronounced with longer immersion durations.

Table 1: Quantitative analysis of grayscale photoacoustic images after 10-minute oil immersion.

Oil Type	Mean Intensity	Standard Deviation	Entropy
Coconut Oil	29.31311	13.63201	5.557476
Sesame Oil	30.43274	17.22834	5.932456
Lard	56.86921	32.05057	6.237956

Table 2: Quantitative analysis of grayscale photoacoustic images after 60-minute oil immersion.

Oil Type	Mean Intensity	Standard Deviation	Entropy
Coconut Oil	34.42379	17.11478	5.75182
Sesame Oil	69.27368	36.26761	6.938029
Lard	83.53925	53.8993	7.137159

Table 3: Quantitative analysis of grayscale photoacoustic images after 24-hour oil immersion.

Oil Type	Mean Intensity	Standard Deviation	Entropy
Coconut Oil	42.52342	27.90184	6.143463
Sesame Oil	50.15585	40.8172	6.365761
Lard	109.7229	73.2925	7.529887

The data in Tables 1 through 3 show a consistent increase in mean intensity, standard deviation, and entropy for lard-treated samples as immersion time increases. This trend indicates progressive structural alteration and enhanced photoacoustic signal heterogeneity, likely resulting from deeper lipid infiltration and chromophore redistribution within the tissue. In contrast, samples treated with coconut and sesame oils display relatively stable values across all durations, suggesting limited optical and structural disruption. These findings quantitatively reinforce the visual differences previously observed and highlight entropy and standard deviation as the most responsive metrics for detecting subtle variations in tissue composition. Their effectiveness underscores the potential of photoacoustic imaging for distinguishing oil treatment history, particularly relevant for developing non-invasive techniques in halal verification or food authentication.

Bar charts in Figure 8, Figure 9, and Figure 10 illustrate the extracted numerical features, mean intensity, standard deviation, and entropy for each oil type and immersion duration. These visualizations highlight a consistent upward trend in all three metrics for lard-treated samples, particularly after 24 hours of soaking, indicating increased optical absorption and greater tissue heterogeneity. In contrast, values for coconut and sesame oil remain comparatively low and stable across all time points, suggesting limited structural impact. These patterns further support the discriminative power of photoacoustic-derived statistics in identifying differences among oil treatments.

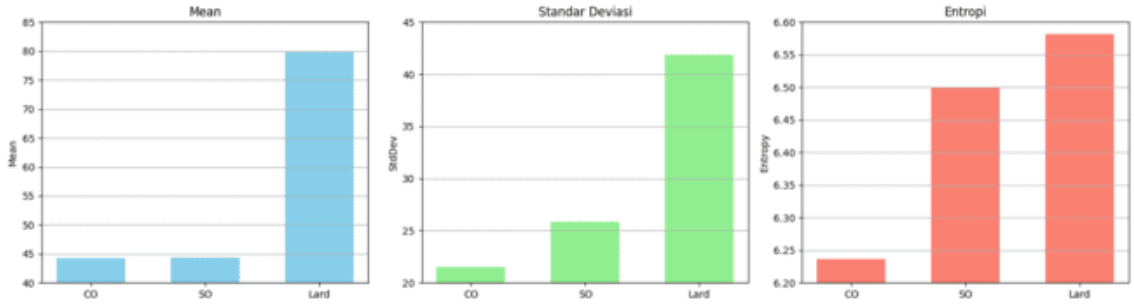

Figure 8: Bar chart of mean intensity values extracted from grayscale photoacoustic images of samples immersed for 10 minutes in coconut oil, sesame oil, and lard.

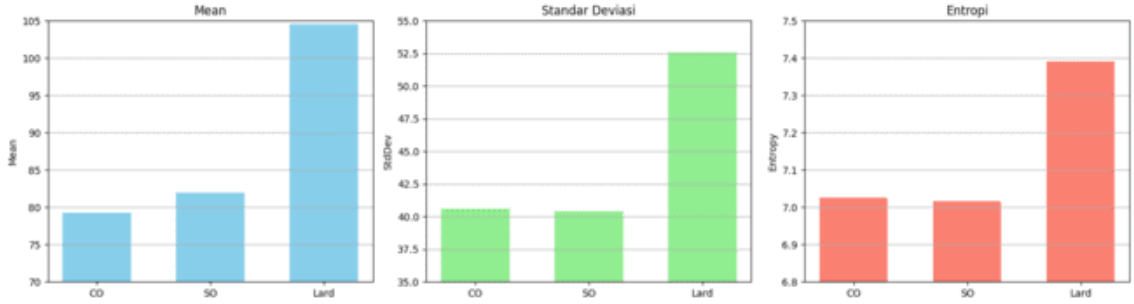

Figure 9: Bar chart of mean intensity values extracted from grayscale photoacoustic images of samples immersed for 60 minutes in coconut oil, sesame oil, and lard.

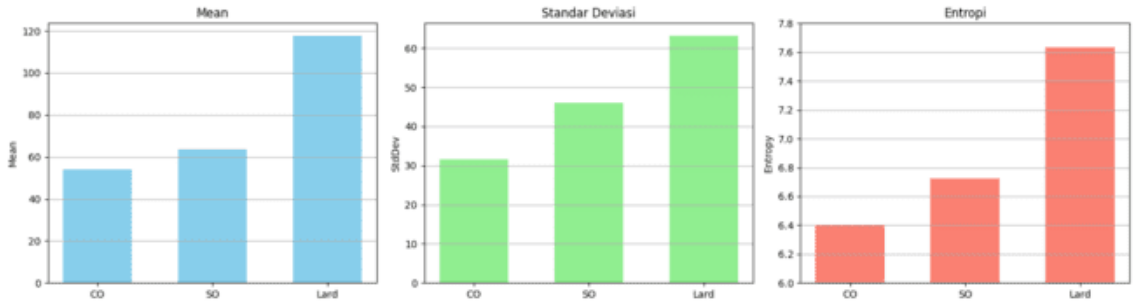

Figure 10: Bar chart of mean intensity values extracted from grayscale photoacoustic images of samples immersed for 24 hours in coconut oil, sesame oil, and lard.

These graphical summaries complement the grayscale images and statistical tables by visually confirming the distinctions among oil treatments. Together, they reinforce the potential of photoacoustic-based image features as reliable indicators for tissue classification, particularly in contexts such as halal product verification.

While global statistical measures provide an overall picture of signal variation, they may overlook localized differences within tissue structure. To address this, local entropy analysis was applied to the grayscale photoacoustic images. This technique evaluates texture complexity within localized pixel neighborhoods, enhancing the ability to detect subtle spatial heterogeneity caused by differential oil absorption. Such localized analysis is particularly valuable in tissue characterization, where oil diffusion can create uneven distribution patterns that are not captured by global metrics alone.

To highlight spatial variations in tissue complexity, High Entropy Area (HEA) maps were generated from each grayscale photoacoustic image. These maps visualize regions

with relatively high local entropy, indicating areas of greater textural complexity that may correspond to deeper oil infiltration or structural alteration. The resulting HEA maps allow for localized comparison of oil-tissue interactions based on both the type of oil and the duration of exposure.

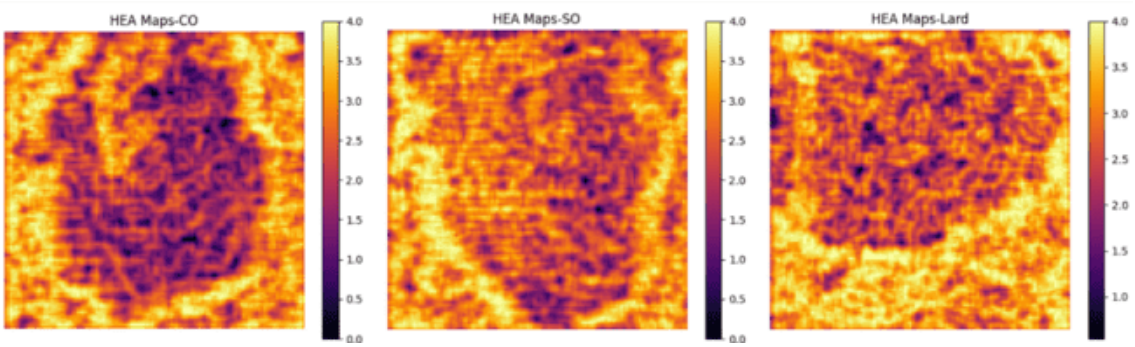

Figure 11: Map chart of mean intensity values extracted from grayscale photoacoustic images of samples immersed for 10 minutes in coconut oil, sesame oil, and lard.

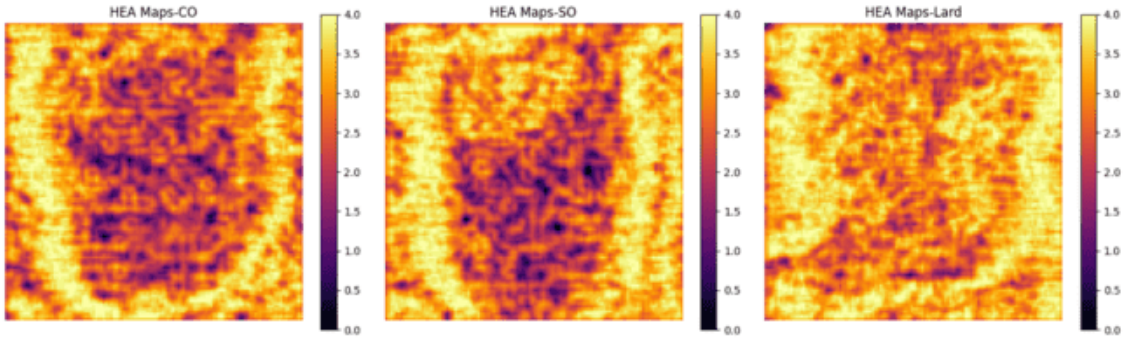

Figure 12: Map chart of mean intensity values extracted from grayscale photoacoustic images of samples immersed for 10 minutes in coconut oil, sesame oil, and lard.

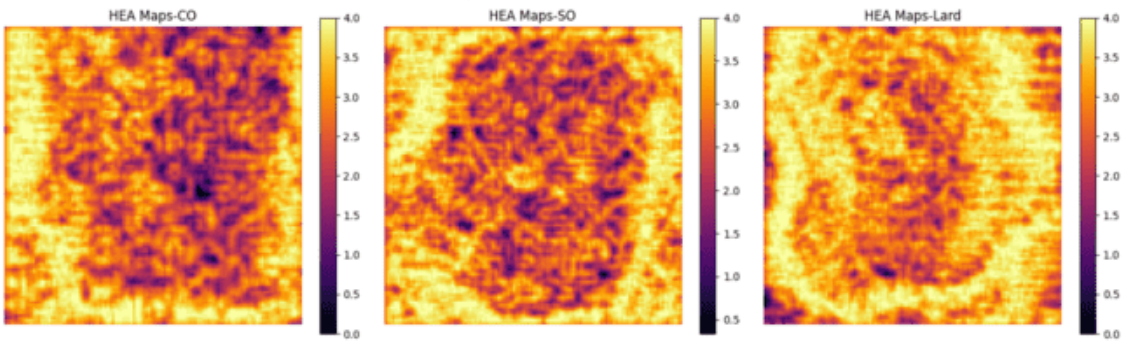

Figure 13: Map chart of mean intensity values extracted from grayscale photoacoustic images of samples immersed for 10 minutes in coconut oil, sesame oil, and lard.

The HEA maps for chicken tissue samples treated with coconut oil, sesame oil, and lard at 10 minutes, 60 minutes, and 24 hours are shown in Figures 11, 12, and 13, respectively. Visually, samples treated with lard consistently display broader and more diffuse high-entropy regions, especially after 24 hours of immersion, as seen in Figure 13. This suggests that lard induces more extensive and heterogeneous interaction with the tissue matrix. In contrast, samples treated with coconut oil and sesame oil tend to show

more localized, symmetric high-entropy zones that remain relatively consistent over time. These patterns reinforce the hypothesis that different oil types produce distinct spatial effects on tissue structure and support the use of local entropy and HEA mapping as sensitive tools for classifying oil-treated meat. Such spatial texture analysis may prove valuable for non-destructive halal verification, particularly in differentiating animal-based and plant-based oils.

These differences can be explained by the inherent physicochemical properties of the oils. Lard, as an animal-derived fat, has a higher content of saturated lipids and distinct protein, lipid interactions compared to the more homogeneous composition of coconut and sesame oils. These properties affect optical absorption, thermal expansion, and acoustic wave generation. Lard's denser lipid matrix likely enhances light absorption and local thermoelastic response, resulting in stronger and more spatially varied acoustic signals. In contrast, the lower absorption and more uniform diffusion behavior of coconut and sesame oil lead to subtler and more stable structural changes in tissue.

The consistency of these observations across grayscale images, statistical descriptors (mean, standard deviation, entropy), and HEA mapping demonstrates that PAI is sensitive to subtle differences in oil composition and diffusion behavior. These findings not only validate the feasibility of using photoacoustic features for oil-type differentiation but also lay the groundwork for developing non-invasive tools for halal product authentication. The integration of global and local image metrics in this study provides a replicable framework for future investigations in food integrity and classification using quantitative photoacoustic analysis.

4. Conclusion

This study demonstrates that photoacoustic imaging (PAI) is capable of detecting structural and optical differences in biological tissues treated with various types of cooking oil. Quantitative analysis of grayscale images, including mean intensity, standard deviation, entropy, and local entropy-based HEA maps, revealed clear distinctions across treatment groups. Tissues exposed to lard consistently exhibited higher values in all metrics, indicating stronger optical absorption and greater tissue heterogeneity due to deeper fat infiltration. In contrast, samples treated with coconut and sesame oils showed more uniform responses over time. The combined use of global and localized image features highlights the potential of PAI as a non-destructive technique for evaluating oil-tissue interactions. These findings provide a solid foundation for developing optical-based methods for halal verification and broader applications in food integrity assessment.

References

Albuquerque, J. E. de, Santiago, B. C. L., Campos, J. C. C., Reis, A. M., da Silva, C. L., Martins, J. P., & Coimbra, J. S. R. (2013). Photoacoustic spectroscopy as an approach to assess chemical modifications in edible oils. *Journal of the Brazilian Chemical Society, 24(3)*, 405–412. doi:10.5935/0103-5053.20130053

Cao, Y., Wang, X., Yang, W., He, Y., Zheng, W., & Luo, Q. (2017). Spectral analysis

assisted photoacoustic imaging for lipid composition differentiation. *Photoacoustics, 7*, 7, 12–20. doi:10.1016/j.pacs.2017.05.002

Franko Hrˇzi´c, Ivan ˇ Stajduhar, Sebastian Tschauner, Erich Sorantin, and Jonatan Lerga. (2019). Local-entropy based approach for x-ray image segmentation and fracture detection. *Entropy*, 21(4):338. doi:10.3390/e21040338

Ghayathri Balasundaram, Yonggeng Goh, Mohesh Moothanchery, Amalina Attia, Hann Qian Lim, Neal C Burton, Yi Qiu, Thomas Choudary Putti, ChingWan Chan, Mikael Hartmann, et al. (2020). Optoacoustic characterization of breast conserving surgery specimens–a pilot study. *Photoacoustics*, 9:100164. doi:10.1016/j.pacs.2020.100164

Guenther Paltauf, Paul R Torke, and Robert Nuster. (2018). Modeling photoacoustic imaging with a scanning focused detector using monte carlo simulation of energy deposition. *Journal of biomedical optics*, 23(12):121607–121607,. doi:10.1117/1.JBO.23.12.121607

Hu, Lihong V Wang and Song. (2012). Photoacoustic tomography: in vivo imaging from organelles. *Science*, 335(6075):1458–1462. doi:10.1126/science.1216210

Mohammed Belkhatir, Shalini Bala, and Noureddine Belkhatir. (2020.). Business process rereengineering in supply chains examining the case of the expanding halal industry. *arXiv preprint*, rXiv:2004.09796. doi:10.48550/arXiv.2004.09796

Paul Beard. (2011). Biomedical photoacoustic imaging. *Interface focus,*, 1(4):602–631. doi:10.1098/rsfs.2011.0028

Qian Zhao, Chang-Zheng Shi, and Liang-Ping Luo. (2014). Role of the texture features of images. *Chinese Journal of Cancer Research*, 26(4):451. doi:10.3978/j.issn.1000-9604.2014.08.07

Ronald P Mensink, Peter L Zock, Arnold DM Kester, and Martijn B Katan. (2003). Effects of dietary fatty acids and carbohydrates on the ratio of serum total to hdl cholesterol and on serum lipids and apolipoproteins: a meta-analysis of 60 controlled trials. *The American journal of clinical nutrition*, 7(5):1146–1155. doi:doi.org/10.1093/ajcn/77.5.1146

Wresni Anggraini, Wakhid Slamet Ciptono, Luluk Lusiantoro, and Heru Kurnianto Tjahjono. (2023). Halal food integrity: Systematic literature review and research agendas. *In Proceedings of the International Conference on Industrial Engineering and Operations Management*.

Yeh, J.-R., Lin, C.-W., & Shieh, J.-S. (2011). An approach of multiscale complexity in texture analysis of lymphomas. *IEEE Signal Processing Letters, 18(4)*, 239–242. doi:10.1109/LSP.2011.2113338

Zhang, Q., Lu, S., Liu, L., Liu, Y., Zhang, J., & Shi, D. (n.d.). (2021). Color enhancement of low illumination garden landscape images. *Traitement du Signal, 38(6)*, 1717–1725. doi:10.18280/ts.380618